Sensors and Actuators B 232 (2016) 698–704

Contents lists available at ScienceDirect

Sensors and Actuators B: Chemical

journal homepage: www.elsevier.com/locate/snb

Influence of hollowness variation on the gas-sensing properties of ZnO hollow nanofibers

Akash Katoch, Zain Ul Abideen, Jae-Hun Kim, Sang Sub Kim*

Department of Materials Science and Engineering, Inha University, Incheon 402-751, Republic of Korea

ARTICLE INFO

Article history:
Received 14 December 2015
Received in revised form 5 March 2016
Accepted 4 April 2016
Available online 5 April 2016

Keywords:
ZnO
Hollow fiber
Hole diameter
Surface area
Gas sensor

ABSTRACT

The influence of hollowness variations on the gas-sensing performance of ZnO hollow fibers (Hfs) was investigated by varying their hole diameter. The hole diameter of the ZnO Hfs was changed using template polymer fibers with various diameters, which were synthesized by electrospinning. Hfs with smaller hole diameters were more sensitive to both reducing and oxidizing gases than those with larger diameters. The improved gas-sensing ability was attributed to the increased surface area of the Hfs due to the smaller hole diameter. The results show that the hole diameter is a key shape parameter and should be accurately monitored to maximize the gas-sensing properties of Hfs; thus, in this paper an important guideline for the use of oxide Hfs in chemiresistive-type gas sensors is provided.

1. Introduction

Chemiresistive-type gas sensors based on oxide hollow fibers (Hfs) are well known for their remarkable gas response; their excellent performance, which is superior to that of sensors fabricated from regular, solid fibers, is due to the doubled surface area provided by the inner and the outer surfaces of the Hfs, which offer more adsorption sites for the surrounding gas molecules [1–4]. Moreover, the control of the population density of the potential barriers established at the interface among the neighboring grains in Hfs is essential to retain the excellent sensing properties of Hfs [5].

A variety of methods, including sol-gel [6,7], sputtering [5], thermal evaporation [8–10], electrochemical process [11], electrospinning [12–14], and template-assisted route [15], have been adopted to synthesize hollow structures. Among them, the polymer template-assisted electrospinning route [5,16,17] has been successfully employed to synthesize Hfs with a controlled hole diameter. In this route, a combination of electrospinning and atomic layer deposition (ALD) techniques is used. First, polymer fibers with a uniform diameter are synthesized by an electrospinning technique. The ALD technique, which is effective for preparing conformal layers on irregular-shaped surfaces, is used to coat the polymer fibers with an oxide material. Subsequently, a suitable heat treatment removes the core polymer fibers, resulting in the formation of hollow oxide fibers.

In a previous investigation [18], the sensing performance of Hfs was found to depend on their wall thickness and the radial modulation of the electron-depletion layer at the inner and outer surfaces was revealed to be responsible for the gas response of Hfs. Particularly, Hfs with thin walls in the order of the Debye length appeared more sensitive toward reducing gases than oxidizing gases. In the presence of reducing gases, the Hfs, electron depleted by pre-adsorbed oxygen species in air, become less resistive because of the electron transfer back to the conduction band of the Hfs; conversely, oxidizing gas molecules cause marginal resistance variations owing to the already electron deficient state due to the pre-adsorbed oxygen species. Accordingly, the wall thickness of the Hfs is an essential parameter that needs to be optimized.

According to recent investigations [19–22], the size of the nanograins and the crystallinity are important factors that greatly influence the electrical and sensing properties of oxide nanofibers. Nanofibers, consisting either of smaller grains or higher crystalline quality, usually show better sensing properties than those either of larger grains or inferior crystalline quality. This suggests that the simultaneous optimization of the grain size and crystallinity is crucial to obtain a superior sensing performance from oxide nanofibers, including Hfs.

Compared to regular, solid fibers, an important microstructural feature of the Hfs is the presence of inner surfaces. The area of the inner surfaces depends on the hole diameter. Hfs with a small hole diameter are expected to have a larger surface area than Hfs with

* Corresponding author.
E-mail addresses: sangsub@inha.ac.kr, sangsub99@gmail.com (S.S. Kim).

http://dx.doi.org/10.1016/j.snb.2016.04.013
0925-4005/

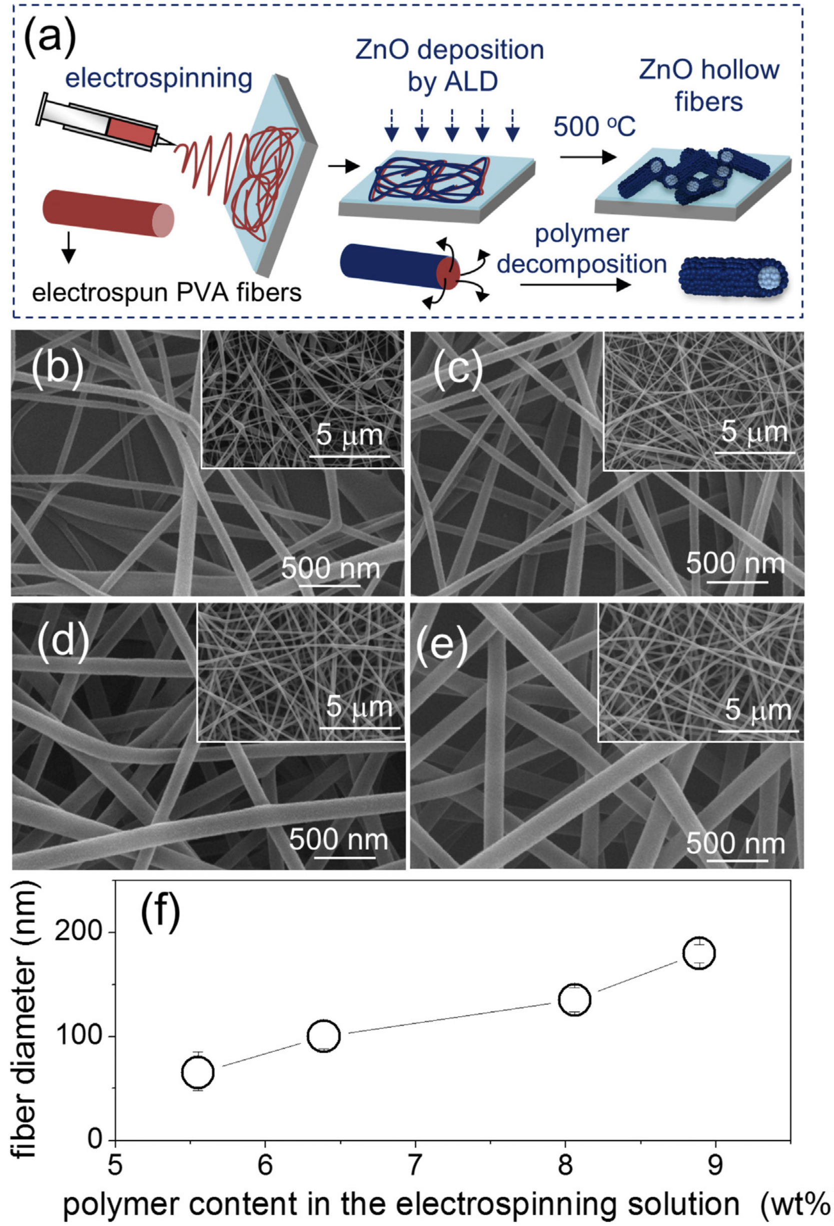

Fig. 1. (a) Schematic of the synthesis of ZnO hollow fibers (Hfs). Field-emission scanning electron microscopy (FE-SEM) images of ZnO Hfs with different hole diameters: (b) 50, (c) 90, (d) 140, and (e) 185 nm. (f) Variation of the diameter of polyvinyl alcohol polymer fibers.

a large hole diameter, providing the possibility of better sensing performance. However, no systematic investigation has been conducted yet to determine the correlation between the hollowness variation and the gas-sensing properties of oxide Hfs.

In this work, for the first time, in the attempt to investigate the influence of the hollowness variation on the gas-sensing performance of Hfs, we have synthesized ZnO Hfs with a range of hole diameters by combining the electrospinning and ALD techniques, while using polymer fibers as templates, and examined their gas-sensing properties as a function of the hole diameter. The Hfs with a small hole diameter revealed superior sensing properties when tested with a reducing gas, owing to the increased surface area. This results provides a useful guideline for the use of oxide Hfs in chemiresistive-type gas sensors.

2. Experimental

ZnO Hfs with various hole diameters were synthesized by a combination of electrospinning and ALD techniques. First, polyvinyl alcohol (PVA) polymer fibers were synthesized by the electrospinning technique. The diameter of the electrospun fibers was controlled by changing the polymer content in the electrospinning solution, while keeping all the other parameters constant. In the second step, ZnO layers were deposited by ALD. Subsequently, the template polymer core fibers were removed by performing a heat treatment at 500 °C in air for 0.5 h. The number of ALD deposition cycles to achieve ZnO Hfs with the same wall thickness of ~60 nm was 700. Fig. 1a presents a schematic diagram of the overall procedure used for the growth of ZnO Hfs. Details of the electrospinning conditions (procedure for the electrospinning solution, applied voltage, distance between the nozzle and the substrate,

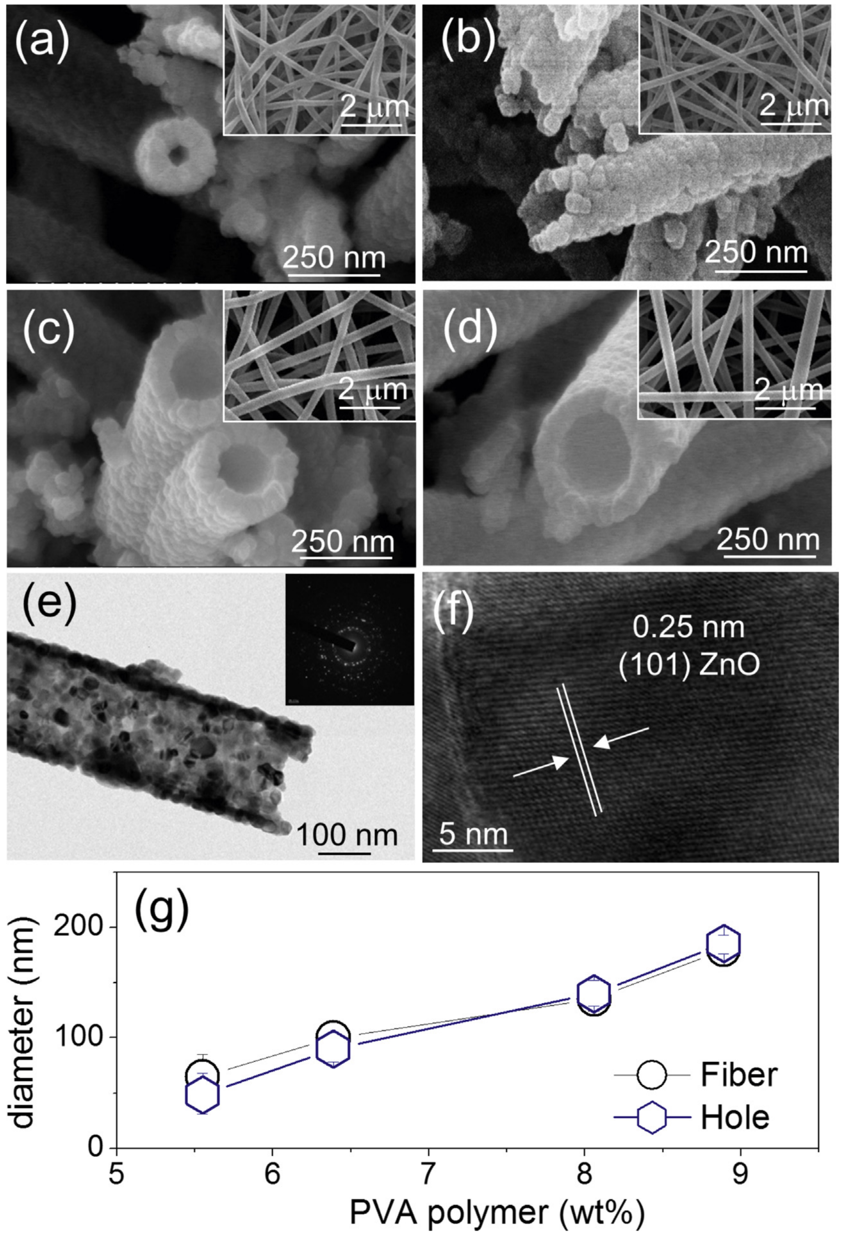

Fig. 2. FE-SEM images of ZnO Hfs with different hole diameters: (a) 50, (b) 90, (c) 140, and (d) 185 nm. (e) Variation of the hole diameter of ZnO Hfs.

etc.) used for the synthesis of the template core polymer fibers and the ALD deposition (precursors and operating procedure for ZnO deposition, etc.) of the ZnO shells have been described in detail elsewhere [18].

The microstructure of the synthesized ZnO Hfs was examined by field-emission scanning electron microscopy (FE-SEM, Hitachi S-4200) and high-resolution transmission electron microscopy (HR-TEM, Jeol/JEM-2100F). The surface area of the ZnO Hfs was characterized using the Brunauer–Emmett–Teller (BET) method.

For the sensing measurements, Ti (~50 nm thick) and Au (~200 nm thick) bilayers were deposited by sputtering Ti and Au targets on ZnO Hfs that had been spread over SiO_2-grown (~200 nm thick) Si (100) substrates using a comb-shape metal mask. The procedure for electrode fabrication is described in detail elsewhere [23,24]. The gas-sensing capabilities of the sensors based on ZnO Hfs were investigated using CO and H_2, and NO_2 as representative reducing and oxidizing gases, respectively. The sensing measurements were performed using a gas dilution and testing system described in detail in earlier reports [25–27]. The measurement temperature was set to 375 °C, which was selected after a series of preliminary experiments. For the sensing measurement, the sensors were kept in a horizontal-type tube furnace which was connected to an electrical measurement system (Keithley 2400) interfaced with a computer. The details of the setup used for the sensing measurements have already been described in one of our earlier studies [23]. The sensors were heated to the operating temperature 375 °C by the tube furnace, not by the Pt heating element usually fabricated by screen printing on the back-side of the sensor substrate. The sensor response (R) was determined using the following equation: $R = Ra/Rg$ or Rg/Ra, where Ra and Rg are the resistances in the absence and presence of the target gas, CO or NO_2, respectively.

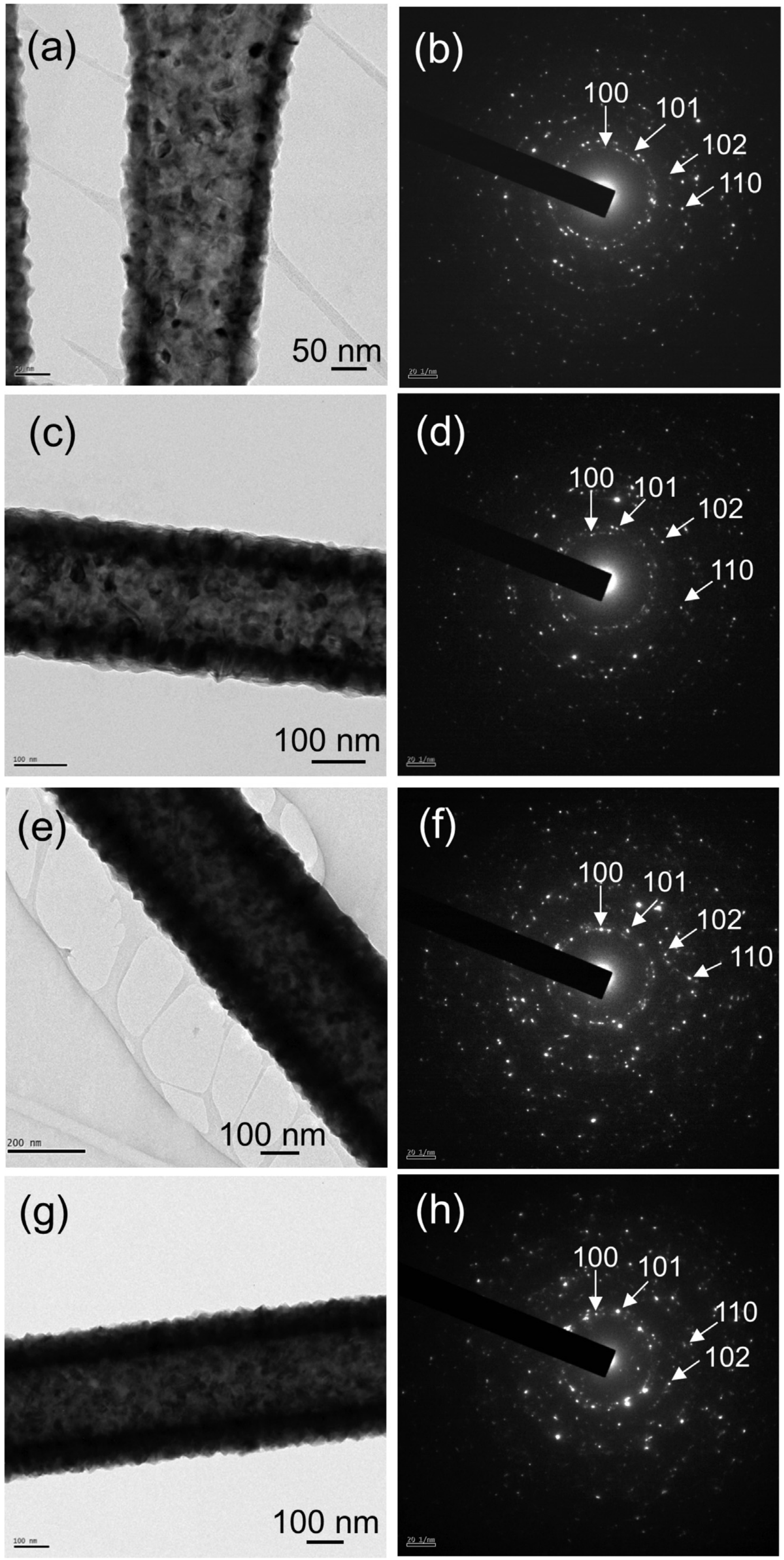

Fig. 3. TEM images and SAED patterns taken from individual ZnO Hfs with various hole diameters: (a) and (b) 50, (c) and (d) 90, (e) and (f) 140, and (g) and (h) 185 nm.

3. Results and discussion

Fig. 1b–e shows typical FE-SEM images of the template PVA polymer fibers with different diameters. The diameter of the polymer fibers was controlled by changing the polymer content in the electrospinning solution, and consequently modifying its viscosity. The insets show the corresponding low-magnification

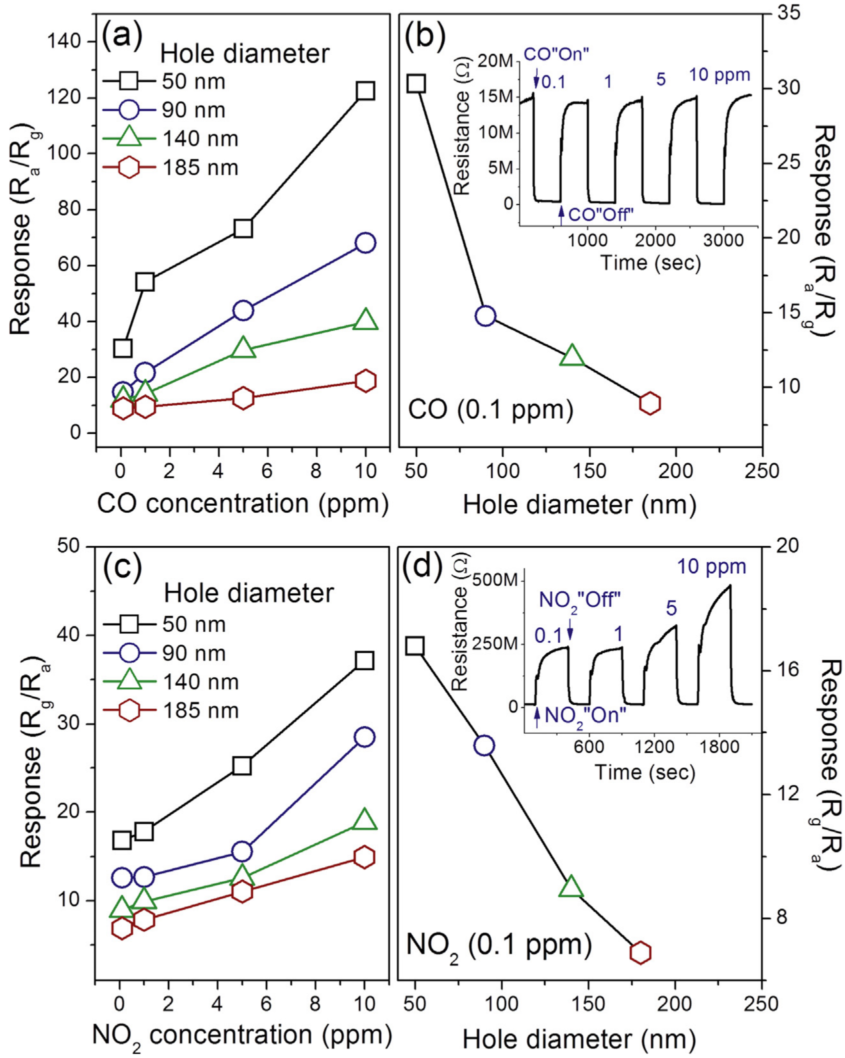

Fig. 4. Responses of ZnO Hfs with different hole diameters to: (a) CO and (c) NO_2 gases. Summary of the relationship between the response of ZnO Hfs and their surface area at 0.1 ppm concentrations of: (b) CO and (d) NO_2 gases. The inset shows the corresponding dynamic resistance curves of ZnO Hfs with the largest hole diameter of 185 nm.

FE-SEM images, which reveal the overall features of the polymer fibers. The diameter of the polymer fibers increased with increasing polymer content, as shown in Fig. 1f. A linear relationship between the polymer content and the diameter of the produced polymer fibers showed that the diameter of the polymer fibers can be controlled on the nanometer scale by properly varying the viscosity of the electrospinning solution; the increase of the viscosity results in thicker polymer fibers.

On these polymer fibers, ZnO layers were deposited by ALD. The core polymer fibers were subsequently removed by the heat treatment, which only left the ZnO shell layers, resulting in the formation of ZnO Hfs. By applying 700 cycles of ALD deposition, Hfs with a wall thickness of ~60 nm were obtained. Fig. 2a–d shows the microstructures of the ZnO Hfs with various hole diameters; the insets show the corresponding low-magnification images revealing a random and uniform distribution of Hfs on the substrate. The hole diameter was changed gradually using polymer core fibers with different fiber diameters. Notably, the Hfs were composed of nano-sized grains, also called nanograins. The role of nanograins in relation to the gas-sensing properties was studied systematically [22,28–30]. The microstructure of the ZnO Hfs was investigated further by TEM, and the results are displayed in Fig. 3. Fig. 3a,c,e, and g presents typical low-magnification TEM images taken from individual ZnO Hfs with different hole diameters. The average grain sizes were evaluated to be 18, 19, 19, and 17 nm for ZnO Hfs with hole diameters of 50, 90, 140, and 185 nm, respectively. This indicates that the grain sizes were similar irrespective of hole diameter. The semi-transparent region with dark boarders indicates the hollow nature of the nanofibers. The selected area electron diffraction patterns (SAEDs) showing ring-shaped spots in Fig. 3b,d,f, and h, clearly indicates the polycrystalline nature of the ZnO Hfs. In a previous investigation [18], the crystalline phase of the ZnO Hfs synthesized under identical conditions was examined by XRD. According to the results [18,19], ZnO Hfs exhibited a hexagonal wurtzite structure of high crystalline quality.

The hole diameter of the ZnO Hfs is summarized in Fig. 2e. The hole diameter showed an almost linear relationship with the polymer content in the electrospinning solution, thereby with the diameter of the template polymer fibers. Notably, the hole diameter of the ZnO Hfs was slightly smaller than the diameter of the polymer fibers, likely because of slight shrinkage of the shell layers along the radial direction of the fibers during the heat treatment process.

The gas-sensing properties of the ZnO Hfs with various hole diameters were measured using typical reducing (CO) and oxidizing (NO_2) gases at concentrations of 0.1, 1, 5, and 10 ppm. Fig. S1 of Supplementary Information shows the dynamic resistance curves of the ZnO Hfs to CO gas. All the sensors clearly track the supply

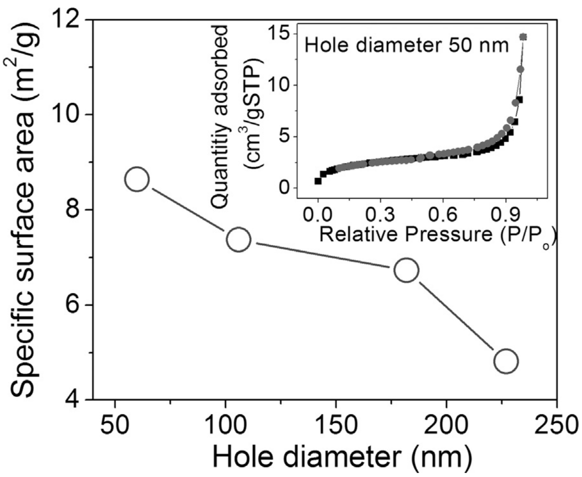

Fig. 5. Summary of the surface area of ZnO Hfs as a function of hole diameter. The inset shows N_2 adsorption–desorption isotherms of ZnO Hfs with 50 nm hole diameter.

and cessation of CO gas. Fig. 4a summarizes the CO response of the ZnO Hfs with various hole diameters. To show more clearly the relationship between the CO response and the hole diameter, the response behaviour of the ZnO Hfs to 0.1 ppm CO is replotted as a function of the hole diameter in Fig. 4b. As the hole diameter increases, the CO response of the ZnO Hfs decreases. As an example, the inset shows the dynamic resistance curve of ZnO Hfs with a hole diameter of 50 nm. Fig. S2 of Supplementary Information shows the dynamic response curves obtained from the ZnO Hfs for NO_2. Fig. 4c presents the corresponding NO_2 responses. In addition, Fig. 4d shows the response behaviour to 0.1 ppm NO_2. Similar to the case of the reducing gas CO, the NO_2 response decreased with increasing hole diameter. The gas sensing measurement for H_2 was also performed and the response curves and responses for 1 ppm H_2 are summarized in Fig. S3 of Supplementary Information. The responses show the same trend as the cases of CO and NO_2, demonstrating that ZnO Hfs with a small hole diameter are favourable to obtain superior sensing properties.

The sensing mechanism operating in the ZnO Hfs can be understood based on *n*-type semiconductors. According to an earlier study [18], the wall thickness of the ZnO Hfs influences their sensing ability significantly. In the current work, radial modulation of the electron-depletion region in the wall must be almost identical for all the samples because Hfs with the same wall thickness of 60 nm were synthesized. Therefore, the effect of the wall thickness on the sensing ability can be excluded. On the other hand, the crystallinity and grain size of the ZnO Hfs may be another important parameter that can affect the sensing ability. In the current study, though the same heat treatment was applied to all the samples, their crystallinity and grain size might be different due to the different inner and outer surface curvatures of Hfs. However, as is obvious from the TEM images shown in Fig. 3, all the Hfs consist of nanograins with similar grain sizes ranging from 17 to 19 nm irrespective of hole diameter. The SAED ring patterns with similar brightness in Fig. 3 for all the ZnO Hfs indirectly suggest that the crystallinity of the Hfs is likely to be similar. In addition, in our earlier work [18], the similar crystallinity and grain size were established in all the ZnO HFs with different wall thicknesses synthesized by using the same conditions used in the current paper. Therefore, the crystalline quality and grain size of the ZnO Hfs can be assumed to be identical irrespective of hole diameter, meaning that both factors can be neglected in interpreting the sensing properties of ZnO HFs with respect to hole diameter.

Therefore, the specific surface area is probably the only factor that can be responsible for the different response behaviours of the Hfs. This is because the change in hole diameter naturally modifies the surface area of the ZnO Hfs. Fig. S4 of Supplementary Information shows the results of BET measurements of the Hfs in relation to the hole diameter. As summarized in Fig. 5, the specific urface area increased with decreasing hole diameter. The inset is the BET curve taken from the Hfs with the hole diameter 50 nm as an example. Accordingly, the stronger sensor response of ZnO Hfs with a smaller hole diameter is more likely to be originated from the larger specific surface area, i.e., the hole diameter of Hfs needs to be optimized to improve the sensing performance. The results suggest that a smaller hole diameter is more advantageous to obtaining superior sensing properties of Hfs. It is of note that all the ZnO Hfs consist of highly densely-packed grains, as is evident from the TEM images in Fig. 3. No considerable gap or void between ZnO nanograins exists. Therefore, it is reasonable to claim that the change in the specific surface area of Hfs mainly originates from the variation of hole diameter. In addition, the response and recovery times for 0.1 ppm CO gas are summarized in Table S1 of Supplementary Information. Notably, the response and recovery times are similar for all ZnO Hfs, regardless of the different hole diameters, indicating that the hole diameter has no significant influence on diffusion kinetics of gas molecules. The hollowness of ZnO HFs was changed by controlling the hole diameter of HFs in this study. According to Figs. 5 and S4 of Supplementary Information, the specific surface area of the HFs with an average hole diameter 50 nm was almost doubled in comparison to ones with 185 nm. We believe that this difference is enough to cause the change in gas response of the HFs in relation to the hole diameter shown in Fig. 4.

The control of morphology is one of important issues in HF's sensing properties. The main purpose of the control of morphology is to increase the specific surface area of HFs, which is one of key materials parameters in chemiresistive-type sensors. Sensor materials with a large specific surface area will experience more resistance change during interaction of gas molecules with the surface of sensor materials. Accordingly, by the increased specific surface area of HFs, improved sensing properties will be expected. In this study, we have controlled the hole diameter of ZnO HFs to increase the specific surface area of HFs and confirmed the small hole diameter results in the larger specific surface area, consequently leading to improved sensing properties.

4. Conclusions

ZnO Hfs were synthesized by combining the electrospinning and ALD techniques. The surface area of the ZnO Hfs was controlled by varying the hole diameter, which was achieved by applying template polymer fibers with various diameters. The effect of the surface area on the gas-sensing performances of the Hfs was investigated using CO and NO_2 gases. The improved gas-sensing ability was attributed to the increased surface area of the Hfs, due to a smaller hole diameter. For the efficient use of oxide Hfs in chemiresistive-type gas sensors, Hfs with a smaller hole diameter will be more advantageous, which is a useful guideline for the application of Hfs in gas sensors.

Acknowledgment

This study was supported by Inha University.

Appendix A. Supplementary data

Supplementary data associated with this article can be found, in the online version, at http://dx.doi.org/10.1016/j.snb.2016.04.013.

References

[1] B. Ding, M. Wang, X. Wang, J. Yu, G. Sun, Electrospun nanomaterials for ultrasensitive sensors, Mater. Today 13 (2010) 16–27, http://dx.doi.org/10.1016/S1369-7021(10)70200-5.

[2] Z.C. Sun, E. Zussman, A.L. Yarin, J.H. Wendorff, A. Greiner, Compound core-shell polymer nanofibers by co-electrospinning, Adv. Mater. 15 (2003) 1929–1932, http://dx.doi.org/10.1002/adma.200305136.

[3] P. Mohanapriya, H. Segawa, K. Watanabe, K. Watanabe, S. Samitsu, T.S. Natarajan, et al., Enhanced ethanol-gas sensing performance of Ce-doped SnO_2 hollow nanofibers prepared by electrospinning, Sens. Actuators, B-Chem. 188 (2013) 872–878, http://dx.doi.org/10.1016/j.snb.2013.07.016.

[4] J.P. Cheng, B.B. Wang, M.G. Zhao, F. Liu, X.B. Zhang, Nickel-doped tin oxide hollow nanofibers prepared by electrospinning for acetone sensing, Sens. Actuators, B-Chem. 190 (2014) 78–85, http://dx.doi.org/10.1016/j.snb.2013.08.098.

[5] S.H. Choi, G. Ankonina, D.Y. Youn, S.G. Oh, J.M. Hong, A. Rothschild, et al., Hollow ZnO nanofibers fabricated using electrospun polymer templates and their electronic transport properties, ACS nano 3 (2009) 2623–2631, http://dx.doi.org/10.1021/nn900126k.

[6] F. Miyaji, S.A. Davis, J.P.H. Charmant, S. Mann, Organic crystal templating of hollow silica fibers, Chem. Mater. 11 (1999) 3021–3024, http://dx.doi.org/10.1021/Cm990449v.

[7] S. Kobayashi, K. Hanabusa, N. Hamasaki, M. Kimura, H. Shirai, S. Shinkai, Preparation of TiO_2 hollow-fibers using supramolecular assemblies, Chem. Mater. 12 (2000) 1523–1525, http://dx.doi.org/10.1021/cm0000907.

[8] W.Z. Xu, Z.Z. Ye, D.W. Ma, H.M. Lu, L.P. Zhu, B.H. Zhao, et al., Quasi-aligned ZnO nanotubes grown on Si substrates, Appl. Phys. Lett. 87 (2005) 093110–093113, http://dx.doi.org/10.1063/1.2035868.

[9] X.H. Zhang, Y. Zhang, J. Xu, Z. Wang, X.H. Chen, D.P. Yu, et al., Peculiar ZnO nanopushpins and nanotubes synthesized via simple thermal evaporation, Appl. Phys. Lett. 87 (2005) 123111–123114, http://dx.doi.org/10.1063/1.2053370.

[10] J. Bae, J. Bin Han, X.M. Zhang, M. Wei, X. Duan, Y. Zhang, et al., ZnO nanotubes grown at low temperature using Ga as catalysts and their enhanced photocatalytic activities, J. Phys. Chem. C 113 (2009) 10379–10383, http://dx.doi.org/10.1021/jp901011u.

[11] J. Su, R. Che, G. She, X. Duan, W. Shi, Transmission electron microscopy of ZnO nanotube arrays etched from electrodeposited ZnO nanorods, J. Nanosci. Nanotechnol. 8 (2008) 6306–6309, http://dx.doi.org/10.1166/jnn.2008.341.

[12] D. Li, Y.N. Xia, Direct fabrication of composite and ceramic hollow nanofibers by electrospinning, Nano Lett. 4 (2004) 933–938, http://dx.doi.org/10.1021/nl049590f.

[13] J. Zhang, S.W. Choi, S.S. Kim, Micro- and nano-scale hollow TiO_2 fibers by coaxial electrospinning: preparation and gas sensing, J. Solid State Chem. 184 (2011) 3008–3013, http://dx.doi.org/10.1016/j.jssc.2011.09.014.

[14] L.L. Wang, X.J. Luo, X.J. Zheng, R. Wang, T. Zhang, Direct annealing of electrospun synthesized high-performance porous SnO_2 hollow nanofibers for gas sensors, RSC Adv. 3 (2013) 9723–9728, http://dx.doi.org/10.1039/c3ra41032c.

[15] R.S. Yuan, X.Z. Fu, X.C. Wang, P. Liu, L. Wu, Y.M. Xu, et al., Template synthesis of hollow metal oxide fibers with hierarchical architecture, Chem. Mater. 18 (2006) 4700–4705, http://dx.doi.org/10.1021/cm0609911.

[16] S. Zhan, D. Chen, X. Jiao, C. Tao, Long TiO_2 hollow fibers with mesoporous walls: sol gel combined electrospun fabrication and photocatalytic properties, J. Phys. Chem. B 110 (2006) 11199–11204, http://dx.doi.org/10.1021/jp057372k.

[17] J. Cao, T. Zhang, F. Li, H. Yang, S. Liu, Enhanced ethanol sensing of SnO_2 hollow micro/nanofibers fabricated by coaxial electrospinning, New J. Chem. 37 (2013) 2031–2036, http://dx.doi.org/10.1039/c3nj00096f.

[18] A. Katoch, S.W. Choi, S.S. Kim, Effect of the wall thickness on the gas-sensing properties of ZnO hollow fibers, Nanotechnology 25 (2014) 455504–455511, http://dx.doi.org/10.1088/0957-4484/25/45/455504.

[19] E. Comini, Metal oxide nano-crystals for gas sensing, Anal. Chim. Acta 568 (2006) 28–40, http://dx.doi.org/10.1016/j.aca.2005.10.069.

[20] S.W. Choi, J.Y. Park, S.S. Kim, Dependence of gas sensing properties in ZnO nanofibers on size and crystallinity of nanograins, J. Mater. Res. 26 (2011) 1662–1665, http://dx.doi.org/10.1557/Jmr.2011.209.

[21] J.W. Kim, V. Augustyn, B. Dunn, The effect of crystallinity on the rapid pseudocapacitive response of Nb_2O_5, Adv. Energy Mater. 2 (2012) 141–148, http://dx.doi.org/10.1002/aenm.201100494.

[22] A. Katoch, G.J. Sun, S.W. Choi, J.H. Byun, S.S. Kim, Competitive influence of grain size and crystallinity on gas sensing performances of ZnO nanofibers, Sens. Actuators, Chem. 185 (2013) 411–416, http://dx.doi.org/10.1016/j.snb.2013.05.030.

[23] S.W. Choi, J. Zhang, A. Katoch, S.S. Kim, H_2S sensing performance of electrospun CuO-loaded SnO_2 nanofibers, Sens. Actuators, B-Chem. 169 (2012) 54–60, http://dx.doi.org/10.1016/j.snb.2012.02.054.

[24] A. Katoch, S.W. Choi, G.J. Sun, S.S. Kim, An approach to detecting a reducing gas by radial modulation of electron-depleted shells in core-shell nanofibers, J. Mater. Chem. A 1 (2013) 13588–13596, http://dx.doi.org/10.1039/c3ta13087h.

[25] S.-W. Choi, J.Y. Park, C. Lee, J.G. Lee, S.S. Kim, Synthesis of highly crystalline hollow TiO_2 fibers using atomic layer deposition on polymer templates, J. Am. Ceram. Soc. 94 (2011) 1974–1977, http://dx.doi.org/10.1111/j.1551-2916.2011.04600.x.

[26] A. Katoch, J.H. Kim, S.S. Kim, TiO_2/ZnO inner/outer double-layer hollow fibers for improved detection of reducing gases, ACS Appl. Mater. Interfaces 6 (2014) 21494–21499, http://dx.doi.org/10.1021/am506499e.

[27] A. Katoch, J.H. Kim, Y.J. Kwon, H.W. Kim, S.S. Kim, Bifunctional sensing mechanism of SnO_2–ZnO composite nanofibers for drastically enhancing the sensing behavior in H_2 gas, ACS Appl. Mater. Interfaces 7 (2015) 11351–11358, http://dx.doi.org/10.1021/acsami.5b01817.

[28] S.W. Choi, J.Y. Park, S.S. Kim, Growth behavior and sensing g properties of nanograins in CuO nanofibers, Chem. Eng. J. 172 (2011) 550–556, http://dx.doi.org/10.1016/j.cej.2011.05.100.

[29] A. Katoch, S.W. Choi, S.S. Kim, Nanograins in electrospun oxide nanofibers, Met. Mater. Int. 21 (2015) 213–221, http://dx.doi.org/10.1007/s12540-015-4319-8.

[30] A. Katoch, S.W. Choi, J.H. Kim, J.H. Lee, J.S. Lee, S.S. Kim, Importance of the nanograin size on the H_2S-sensing properties of ZnO–CuO composite nanofibers, Sens. Actuators, B-Chem. 214 (2015) 111–116, http://dx.doi.org/10.1016/j.snb.2015.03.012.

Biographies

Akash Katoch received his B.S. degree from Himachal Pradesh University, India in 2004. In 2006, he received his M.S. degree in Applied Physics from Kurukshetra University, Kurukshetra, India. He received his M. Tech. degree in Material Science & Engineering from Thapar University, India, in 2009. In 2014, he received his Doctoral degree from Inha University, Republic of Korea. He worked as postdoctoral fellow from 2014 to 2015 In Inha University. From 2015 onwards he has been an Assistant Professor at Seokyeong University, Republic of Korea. He has been working on chemiresistive gas sensors synthesized by the sol-gel process, electrospinning and VLS method.

Zain Ul Abideen was born in 1990 in Attock, Pakistan. He received his B.S. (Materials Engineering) from Ghulam Ishaq Khan Institute of Engineering Sciences and Technology (GIK Institute), Pakistan in June 2014. He is currently a graduate student pursuing his research at Inha University, South Korea under the supervision of Professor Sang Sub Kim since September 2014. His research interests focus on the synthesis and characterization of composite nanomaterials, metal oxide based semiconductors and their applications in chemical sensors.

Jae-Hun Kim received his B.S. degree from Gyeongsang National University, Republic of Korea in 2013. In February 2015, he received M.S. degree from Inha University, Republic of Korea. He is now working as a Ph. D. candidate at Inha University, Republic of Korea. He has been working on oxide nanowire gas sensors.

Sang Sub Kim joined the School of Materials Science and Engineering, Inha University, in 2007 as a full professor. He received his B.S. degree from Seoul National University and his M.S and Ph.D. degrees from Pohang University of Science and Technology (POSTECH) in Material Science and Engineering in 1987, 1990, and 1994, respectively. He was a visiting researcher at National Research in Inorganic Materials (currently NIMS), Japan for 2 years each in 1995 and in 2000. In 2006, he was a visiting professor at Department of Chemistry, University of Alberta, Canada. In 2010, he also served as a cooperative professor at Nagaoka University of Technology, Japan. His research interests include the synthesis and applications of nanomaterials such as nanowires and nanofibers, functional thin films, and surface and interfacial characterizations.